

# Demersal fish biomass declines with temperature across productive shelf seas

Daniël van Denderen<sup>1</sup>, Aurore Maureaud<sup>2</sup>, Ken Andersen<sup>3</sup>, Sarah Gaichas<sup>4</sup>, Martin Lindegren<sup>3</sup>, Colleen Petrik<sup>5</sup>, Charles Stock<sup>6</sup>, and Jeremy Collie<sup>7</sup>

<sup>1</sup>Danmarks Tekniske Universitet Institut for Akvatiske Ressourcer

<sup>2</sup>Rutgers College

<sup>3</sup>Technical University of Denmark

<sup>4</sup>National Oceanic and Atmospheric Administration

<sup>5</sup>Affiliation not available

<sup>6</sup>NOAA

<sup>7</sup>University of Rhode Island

January 3, 2023

## Abstract

Fish community biomass is generally thought to decline with increasing temperature due to higher metabolic losses resulting in less efficient energy transfer in warm-water food webs. However, whether these metabolic predictions explain observed macroecological patterns in fish community biomass is virtually unknown. Here we test these predictions by examining the variation in demersal fish biomass across 21 productive shelf regions using high-resolution monitoring data from the North Atlantic and Northeast Pacific. We find that biomass per km<sup>2</sup> varies 40-fold across regions and is highest in cold waters and areas with low fishing exploitation. We find no evidence that temperature change has impacted biomass within marine regions over time. Yet, the cross-regional patterns suggest that long-term impacts of warming will be negative on biomass. These results provide an empirical basis for predicting future changes in fish community biomass and its associated services for human wellbeing i.e., food provisioning, under global warming.

## Introduction

Climate change affects marine ecosystems through multiple drivers, including changes in ocean productivity and temperature (Kwiatkowski *et al.* 2020). These changes are expected to alter fish distributions and abundances and eventually impact the structure and functioning of marine ecosystems, as well as their associated services for human wellbeing (Lotze *et al.* 2019; Petrik *et al.* 2020; Tittensor *et al.* 2021). To anticipate and adapt to the ecological consequences of climate change, it is therefore important to better understand and predict how changes in ocean productivity and temperature jointly affect fish production and biomass.

Current model predictions of climate impacts on fish often rely upon basic ecological theories of how energy flows from primary producers to top predators, as well as metabolic scaling of individual vital rates with temperature. Specifically, warmer temperatures are expected to accelerate most physiological rates, e.g. maximum consumption rate and metabolic rate, and, consequently, the turnover rate of biomass (Gillooly *et al.* 2001; Brown *et al.* 2004). The increase in metabolic rate with temperature is further expected to increase the fraction of energy that is lost through respiration. Consequently, the increasing metabolic costs constrain the amount of energy that flows towards the upper trophic levels of food webs by lowering the efficiency by which primary production is converted into fish biomass (Eddy *et al.* 2021).

The effect of temperature on the bioenergetics at least partly underlies projected trophic amplification of productivity, whereby fractional changes in primary production are amplified up through the trophic levels (Lotze *et al.* 2019). Since marine fish dominate the upper trophic levels of ocean food webs worldwide (Hatton *et al.* 2022), it can further be expected that the effects of temperature on both turnover rate and trophic transfer efficiency will drive, at least in part, large-scale latitudinal variation in total fish community biomass. More specifically, it can be hypothesized that fish community biomass should increase from the tropics to the poles due to a lower turnover rate and more efficient energy transfer in cold-water environments. This hypothesis is endorsed by theoretical and laboratory studies (O’Connor *et al.* 2009; Guet *et al.* 2020) and by some empirical studies demonstrating negative relationship between temperature and fish community biomass (Maureaud *et al.* 2019). However, empirical support based on large-scale observational studies across a pronounced temperature gradient is lacking.

There are several potential reasons why such macroecological patterns in fish biomass have not yet been documented. Firstly, fish communities worldwide have been exposed to long-term commercial fishing that changes total community biomass, as well as the underlying size- and trophic structure of fish communities (Rice & Gislason 1996; Myers & Worm 2003; Andersen 2019). Consequently, the exploitation history may mask potential temperature effects. Secondly, energy flows from primary producers to fish may be context- or scale-dependent, especially since some regional variations in energy flows may themselves be driven by temperature. Notably, warmer regions may have increased stratification and remineralization of detritus in the water column (Pomeroy & Deibel 1986; Laufkötter *et al.* 2017), which increases pelagic production, but lowers the detritus flux reaching the seafloor. This in turn limits the energy available to support benthic prey production and the biomass of bottom-feeding (demersal) fish (van Denderen *et al.* 2018). Lastly, most previous studies focused on the more easily estimated community catch rather than the more difficult to measure community biomass (Friedland *et al.* 2012; Stock *et al.* 2017). Most fish data collection of biomass primarily serves to monitor trends and fluctuations in population-level abundances (especially of commercially important species for fisheries management purposes), while less attention is given towards representing overall community composition and biomass (but see, for example, Maureaud *et al.* (2019) and Gislason *et al.* (2020)). Taken together, data limitations and the inter-dependencies between predictor variables may have complicated detecting overall relationships between ocean productivity, temperature and fish community biomass.

In this study, we perform a large-scale empirical investigation of the macroecological patterns and drivers of fish community biomass using an extensive collection of scientific bottom-trawl surveys sampled across pronounced temperature gradients in the North Atlantic and Northeast Pacific. The studied continental shelf regions account for about 15% of global fisheries catch (Watson 2017). We find that temperature is a main driver of large-scale latitudinal variation in demersal fish community biomass. This result is likely driven by a reduced trophic transfer efficiency and a faster turnover rate of fish biomass in warmer waters. As expected, demersal fish biomass is negatively related to fishing exploitation and positively related to zooplankton prey production. All these findings are consistently observed across the different spatial scales studied.

## Method

### Method overview

We compiled bottom trawl survey data of fish biomass across marine ecosystems in the North Atlantic and Northeast Pacific. We analyzed the effect of temperature, and other environmental variables, on fish community biomass in four different ways. Using structural equation modelling, we examined whether relationships between net primary production and demersal fish community biomass are mediated by temperature, food-web structure, and the level of fishing exploitation. Subsequently, we used an explicit trophodynamic modelling framework to compare and explore the robustness of our empirical results and relate it to past investigations of fisheries catch (Friedland *et al.* 2012; Stock *et al.* 2017). Both analyses are focused on the drivers of cross-regional variation in fish community biomass and are performed at large geographic scales. In a third analysis, we used wavelet-revised model regression to analyze finer-scale fish biomass variability, both across and within ecosystems. Lastly, we examined the effect of temperature on fish biomass within

ecosystems over time using different recursive biomass and surplus production models.

### Scientific trawl survey data

Scientific bottom trawl surveys, primarily sampling demersal commercial species, were obtained from the Northeast Pacific and North Atlantic shelf regions. All data used are publicly available and were downloaded in July 2021 (see Appendix S1 for details on data processing). We selected all scientific surveys that sampled the fish community with otter trawls. For each tow in each survey, we selected all demersal teleost and elasmobranch species and obtained species weight. We corrected these weights for differences in sampling area (in km<sup>2</sup>) and trawl gear catchability to obtain a standardized fish biomass across hauls and surveys. We estimated sampling area using information on wingspread, speed of vessel and tow duration. Weights were corrected for trawl gear catchability using information for 80 species in the Northwest Atlantic (Link *et al.* 2008) and 128 species and 7 functional groups in the North Sea (Walker *et al.* 2017). The adjustments resulted in biomass estimates per unit area in metric tonnes (1000 kg) per km<sup>2</sup>.

We compared the corrected trawl survey biomasses with available fisheries stock assessment biomasses to validate the range and distribution of the biomass estimates. To this end, we calculated spatial overlap between the surveyed area and the bounding region of all fisheries assessment areas from the RAM Legacy database (Ricard *et al.* 2012). For each area that overlapped at least 50% with the surveyed area, we compared biomass of each assessed stock with the gear-corrected trawl survey biomass for the corresponding species. The comparison shows that the corrected biomass has a reasonable match with the stock assessment biomass and no apparent bias, for most of the 120 stocks in the Atlantic and Pacific (Figure S1.3). This finding improves confidence that the gear-corrected trawl survey estimates, hereafter termed demersal fish biomass and/or demersal community biomass, are representative and comparable across areas and surveys.

Using the individual haul coordinates, we estimated an average demersal community biomass, in tonnes per km<sup>2</sup>, per equal area grid cell (6000 km<sup>2</sup>) and surveyed year. To reduce the effect of potential outlying biomass estimates, we removed all individual observations 1.5 times less/greater than the interquartile range per survey and year based on log-transformed biomass values (but note that the overall conclusions are robust with or without such a data removal, not shown).

### Analysis of spatial patterns in biomass across geographic scales

We analyzed the spatial patterns in demersal fish biomass for relationships with environmental and anthropogenic drivers at three spatial scales (ecoregion  $n = 21$ , subdivision  $n = 45$  and grid cell  $n = 1083$ , Appendix S2, Figure S2.1), and using average demersal fish biomass data from three time periods (1990-1995, 2000-2005 and 2010-2015; note that all data is used in the time series analysis). For the ecoregion and subdivision scale, we used a structural equation model (SEM), which is a multivariate analysis to describe a network of causal relationships (Grace 2006). The network links were inspired by recent modelling predictions of demersal fish biomass based on a trait-based food-web model (Petrik *et al.* 2019; van Denderen *et al.* 2021). As such, we hypothesized that relationships between net primary production and demersal fish community biomass are mediated by pelagic and benthic secondary production. Following the rationale laid out in the Introduction and Figure S2.2, we further hypothesized that demersal fish biomass declines with increasing temperature, fishing exploitation and the mean trophic level of the community. Lastly, we expected seafloor depth to have an indirect effect on demersal fish biomass by changing the flux of detritus to the benthos (Figure S2.2). SEM analyses were performed using the package ‘Lavaan’ in R (Rosseeel 2012). Since ecoregions/subdivisions varied in their characteristics, multiple sensitivity analyses were performed to test for potential effects of differences in e.g., the number of grid cells and sampled depth range (Appendix S3, Figure S3.1-2).

We further analyzed spatial changes in demersal community biomass at the grid cell level. This analysis was not done with SEM, as we expect our hypothesized causal structure to differ at more local spatial scales, i.e. effects of fisheries may vary with depth and prey productivity within each region. We used wavelet-revised model regression (Carl & Kühn 2010) to explain finer-scale “within region” variability in demersal fish biomass from the same set of predictor variables included in the SEM. Wavelet-revised model regression is designed for regular grid-based data while accounting for spatial autocorrelation and non-stationarity (i.e.

spatial autocorrelation may vary across regions). This may be important for fish distributions due to biotic and abiotic differences across marine regions that could affect fish movement patterns, e.g. Windle *et al.* (2010). The spatial analysis at the individual grid cell level was done for the same three time periods as the SEM. Both biomass and the exploitation rate (catch/biomass) were  $\log_{10}$  transformed. Since a few grid cells had zero catch, we added a small quantity (1 kg per  $\text{km}^2$  per year) to avoid taking the log of zero. Model fits were assessed using the Akaike Information Criterion (AIC) and the model with the lowest AIC was selected as best candidate. When other candidate models had a difference of 0–2 AIC units, we concluded that models were essentially equivalent and the model with the fewest parameters was selected. The analyses were performed using the package ‘spind’ in R (Carl *et al.* 2018).

The set of environmental variables used as predictors in both the SEM and wavelet-revised model regression was compiled from several sources. Seafloor depths were measured in 96% of the survey hauls and extracted for the remaining hauls, using the haul coordinates, from bathymetric data per  $1/12^\circ$  grid from the ETOPO1 Global Relief Model with sea ice cover (Amante & Eakins 2009). Temperatures were estimated using the COBE sea surface temperature data per  $1^\circ$  grid and year ([www.esrl.noaa.gov/psd/data/gridded/data.cobe.html](http://www.esrl.noaa.gov/psd/data/gridded/data.cobe.html)). Data on bottom temperatures was not available for the entire time series but was used to verify some of our results (Appendix S3, Figure S3.3-4). Fish mean trophic level (*MTL*), describing the biomass-weighted mean trophic level of the community, was calculated from the survey data using species-specific trophic level information (Froese & Pauly 2018; Beukhof *et al.* 2019). Fishing exploitation rates were estimated by dividing annual fisheries catch of demersal fish with demersal fish survey biomass. Fisheries catch data, available on a 30-minute spatial grid, were obtained from Watson (2017) and estimated as the sum of fisheries landings, illegal, unregulated and unreported catch and discards at sea. Net primary production was obtained from the cafe algorithm using MODIS data per  $1/6^\circ$  grid and averaged between 2005 and 2010 (<http://www.science.oregonstate.edu/ocean.productivity>) (Silsbe *et al.* 2016). Estimates of pelagic and benthic secondary production were based on output of GFDL’s Carbon, Ocean Biogeochemistry and Lower Trophics (COBALT) ecosystem model from a climatology of the global earth system model (ESM2.6) representative of the contemporary ocean under 1990 greenhouse gas concentrations (Stock *et al.* 2014, 2017). Simulated mesozooplankton biomass and productivity in ESM2.6 broadly captures observed and estimated contrasts across Large Marine Ecosystems (Stock *et al.* 2017), and the energy available to fish through this pelagic pathway can be estimated as mesozooplankton production not consumed by other mesozooplankton ( $Z_{flux}$ ). ESM2.6-COBALT also simulates the detrital flux that reaches the seafloor, which is used as a proxy for benthic secondary production ( $D_{flux}$ ). For all the predictor variables described above, we obtained an estimate per area and year, averaged for each time period, with the exception of net primary production and pelagic and benthic secondary production where a fixed mean value was used due to data limitations and uncertainties in the estimated values over time.

In order to compare and explore the robustness of our empirical SEM results, we used a trophodynamic model to predict demersal fish biomass for each subdivision and ecoregion. We compared these with the observed estimates using linear regression and obtained the explained variance ( $R^2$ ) and Root Mean Square Error (RMSE). In the trophodynamic model, modified from Stock *et al.* (2017), we assumed that energy flux into the fish community is in equilibrium with the fisheries harvest out of the community after accounting for food chain length variations and trophic transfer efficiency. Demersal fish biomass  $B$  in each region  $i$  can then be estimated by dividing the flux with the observed fisheries exploitation rate ( $ER$ ):

$$B_i = (D_{flux,i} \times TE_i^{MTL_i-1} + p_i \times Z_{flux,i} \times TE_i^{MTL_i-2.1}) / ER_i \text{ eq. 1}$$

Following the approach of Pauly & Christensen (1995) and Stock *et al.* (2017), zooplankton were assigned to trophic level 2.1 and detritus to 1, such that the number of trophic steps separating the zooplankton/detritus flux ( $Z_{flux}$  and  $D_{flux}$ ) from the fisheries catch was estimated by *MTL* minus 2.1 or 1. We further assumed that only part of the zooplankton production is available to demersal fish and this fraction is proportional to  $p$ , which is estimated as the fraction of demersal fish catch relative to total fish catch in each region. The value of  $p$  was obtained from Watson (2017). The final parameter is the trophic transfer efficiency ( $TE$ ). This parameter controls the decay of energy between trophic levels and was varied from 0.05 to 0.15 (Eddy *et al.*

2021). Additionally, we varied the thermal sensitivity ( $Q_{10}$ ) of  $TE$  from 0.2 to 2.5:  $TE_i = TE \cdot Q_{10}^{\frac{T_i - 10}{10}}$ , with  $T$  being the average temperature in each region  $i$ .

### Analysis of temporal biomass variation in ecoregions

We examined whether the changes in demersal fish biomass with temperature, as observed in the SEM and WMR spatial analyses, also drive biomass changes in ecoregions over time. We estimated the influence of temperature on demersal community biomass and production by fitting different recursive biomass and surplus production models to the data (see Table 1 for model details). We used different models to vary how temperature may affect the demersal fish community. In each model, ecoregion was included as a random effect and fishing catch was treated as an offset. The temperature term was centered on the mean temperature per ecoregion (obtained from the COBE sea surface temperature data but see Figure S3.4) to limit our analysis to temperature changes within each region. We scaled biomass and production to the maximum biomass per ecoregion. We evaluated each model with/without a temperature term using AIC, where a model with temperature was considered the most parsimonious if it is at least 2 AIC units lower.

### Data availability

The scripts and data can be found on [https://github.com/Dvandenderen/DemFish\\_tract](https://github.com/Dvandenderen/DemFish_tract). The data processing scripts are modified based on earlier work from Pinsky *et al.* (2013) and Maureaud *et al.* (2019). The final dataset contains 180,000 unique tows and includes data from 1970 to 2019. The processed dataset will be stored on a data archive upon manuscript acceptance.

### Results

Demersal fish biomass was highest in the northern regions of the Northeast Pacific (Gulf of Alaska, Eastern Bering Sea and Aleutian Islands) and Northeast Atlantic (Barents Sea and Norwegian Sea) (Figure 1a). Conversely, demersal fish biomass was lowest in the Gulf of Mexico and temperate regions of the North Atlantic (Baltic Sea, southern North Sea, Gulf of Saint Lawrence).

At the ecoregion scale, Pearson correlations between demersal fish biomass and temperature (Figure 1b,  $r = -0.54$ ), fishing exploitation (Figure 1c,  $r = -0.34$ ), net primary production (Figure 1d,  $r = -0.40$ ) and detrital bottom flux ( $r = -0.33$ ) were negative, while depth correlated positively with biomass ( $r = 0.23$ ). Demersal fish biomass had no correlation with zooplankton production ( $r = 0.04$ ) and mean trophic level ( $r = -0.04$ ). Whether the correlations with biomass were direct effects of the predictor variable or indirect effects governed by other predictor variables were examined with the SEM.

Including all predictors resulted in a SEM that was too complex for the available number of observations at the ecoregion scale to assess goodness-of-fit (Figure S2.2). Hence, we simplified the full model by removing the detrital bottom flux, which had an insignificant relation with biomass in 6 out of 6 runs (2 spatial scales  $\times$  3 time periods). We also removed depth, which became irrelevant for the SEM network after removing the detrital bottom flux. The final model, including the remaining five predictors, had a mean  $X^2$  of 6.02 (standard deviation from the 6 runs is 2.4) with 6 degrees of freedom, and p-values ranging between 0.21 and 0.88, indicating that our hypothesized causal structure is supported by the data (an insignificant result indicates good model fit).

Among the individual pathways, demersal fish biomass at the ecoregion and subdivision scale was negatively related to temperature, fishing exploitation and mean trophic level and positively related to zooplankton production (Figure 2). The pronounced spatial variation in demersal fish biomass was reasonably well explained (mean  $R^2 = 0.59$ ) with no clear spatial pattern in the residuals (Figure S2.3). The effects of temperature and fishing were almost equally strong (Figure S2.4). For most other pathways, the directionality conformed with the initial expectations (Figure 2 vs Figure S2.2). A partial effect size plot showed that demersal fish biomass is approximately twice as high with a decline in temperature from 15 to 5°C and a decline in exploitation rate from 0.3 to 0.03, whereas the effect of mean trophic level and zooplankton production on biomass were more variable (Figure 3).

Similar to the SEM analyses, the grid-cell analysis using wavelet-revised model regression showed a negative relationship between demersal fish biomass and fishing exploitation and temperature, while zooplankton had a positive relationship with biomass for all three time periods (Table 2). In contrast to the previous analysis, the detrital bottom flux, which was excluded in the SEM, had a mixed effect on biomass (positive in one period and negative in the two others). Mean trophic level was not part of the best candidate model in any of the time periods.

The best fit between observed and predicted demersal fish biomass with the trophodynamic model (i.e., eq. 1) was obtained with a trophic transfer efficiency of 0.075 and a  $Q_{10}$  temperature scaling of trophic transfer efficiency between 0.4 and 0.7 (Figure 4, S2.5), implying that trophic transfer declines with increasing temperature. Replacing the temperature dependent trophic transfer efficiency with a single mean value sharply reduced the  $R^2$  of the trophodynamic model from 0.66 to 0.42. Furthermore, replacing the exploitation rate in eq. 1 with a single mean value and refitting led to an  $R^2$  of 0.55. The results of the trophodynamic model are thus consistent with the SEM in suggesting temperature-linked trophodynamic effects, i.e., a trophic transfer efficiency decrease with increasing temperature, and exploitation rates as the primary drivers of demersal fish biomass across the range of systems considered.

Finally, we found no evidence that temporal changes in temperature have impacted demersal community biomass within ecoregions during the period 1980-2015 (Table 1). All models with and without a temperature term differed less than 2 AIC units. The models without the temperature term were therefore selected as best candidate as they have the fewest parameters.

## Discussion

Our study supports the hypothesis that temperature is a main driver of large-scale latitudinal variation in fish community biomass. This result is likely driven by a reduced trophic transfer efficiency and a faster turnover rate of fish biomass in warmer waters. As expected, demersal community biomass is negatively related to fishing exploitation and positively related to zooplankton prey production. All these findings are consistently observed across the different spatial scales studied. We find no evidence that temperature fluctuations and recent warming have impacted demersal community biomass. Even though we found no effect of recent warming, our study provides an empirical basis for long-term climate predictions and suggests a set of explanatory variables that are most important.

The lack of a relationship between demersal fish biomass and the detrital bottom flux and the positive but weak relationship between zooplankton prey production and demersal fish biomass in the SEM were unexpected, as prey production should ultimately constrain the energy available to fish. From a trophodynamic perspective, the weak relationship between prey production and biomass and the strong relationship with temperature suggests that temperature-modulated impacts on fish turnover rates and/or trophic transfer efficiencies are more important than the baseline prey resources in determining demersal fish biomass, at least for the range of systems and scales considered here. This finding is supported by the trophodynamic model, which required a strong negative relationship between the transfer efficiency and temperature to obtain skillful demersal fish biomass predictions.

In retrospect, the weak relationship with prey production is not too surprising as the data compilation covers a considerable thermal range (-1 to 27 °C), while the studied shelf systems have moderate to high productivity and productivity varies less than a factor 4 (Figure 1d). It is thus expected that prey production could become more important for predicting changes in demersal fish biomass in both the SEM and the trophodynamic model along a broader productivity gradient. For example, a gradient from the shelf to the deep ocean that covers larger differences in benthic prey production (Wei *et al.* 2011).

It is important to note that the negative relationship between demersal fish biomass and temperature does not necessarily imply that the potential sustainable fishing catch will be lower in warmer shelf systems. Catch is a flux (biomass removed per unit time) similar to production and is differently affected by temperature compared to biomass. Increased biomass turnover times at higher temperatures, for example, decreases the biomass associated with a given production after warming, e.g., du Pontavice *et al.* (2021). In contrast

with the demersal fish biomass results herein, estimates of plankton food web production available to fish can provide moderately skillful fisheries catch predictions at a global scale (Friedland *et al.* 2012; Stock *et al.* 2017). Similar to the demersal fish biomass results herein, a strong negative dependence between the transfer efficiency and temperature significantly improved fisheries catch estimates (Stock *et al.* 2017).

### Climate predictions of marine fish

Global climate model simulations of marine fish typically project declines in fish community biomass ranging between 5 to 15% depending on the climate scenario (Tittensor *et al.* 2021). Most of these fish community models have a temperature scaling of metabolic and feeding rates that is approximately doubled each 10°C increase ( $Q_{10}$  of 2). Since fish community biomass is inversely related to the effect of temperature on individual rates, biomass declines as temperature increases. Both our SEM and trophodynamic model findings support this parametrization.

The above parametrization of metabolic and feeding rates is naturally a simplification of temperature effects on fish physiology. Studies have indicated that the temperature scaling of feeding rates is typically lower than the scaling of metabolic rates (Vucic-Pestic *et al.* 2011; Rall *et al.* 2012), as implemented in some global fish models (Cheung *et al.* 2013; Petrik *et al.* 2019). The lower temperature scaling of feeding rates reduces the fraction of energy that is available for fish growth in warmer waters. As a consequence, average fish growth increases less along a temperature cline than the expected increase in metabolism (van Denderen *et al.* 2020). So far, it has been difficult to predict how such temperature scaling at the individual level translate to the overall community. Our empirical results provide evidence indicating that demersal community biomass is equally constrained by temperature.

We observed no changes in demersal fish biomass that were correlated with temperature over the time period of the survey data. Temperature and fisheries catch fluctuate in time and fish populations may have lagged responses to both. We therefore expect that the observed variations in temperature were too small to reveal a signal, at least during the study period. Other studies reporting changes in fish populations and communities under recent warming investigated species-specific responses in recruitment, productivity and/or distributional changes, as well as shifts in the trait-composition of the fish community (Pinsky *et al.* 2013; Frainer *et al.* 2017; Free *et al.* 2019; Friedland *et al.* 2020). The latter are likely more sensitive to environmental changes than demersal community biomass, as these trait-based metrics account for changes in both composition and relative abundances of individual species.

### The role of fishing

The Northeast Atlantic region was found to have the highest fisheries exploitation rates, whereas Aleutian Islands and Barents Sea had the lowest rates (Figure S2.7). This finding is consistent with previous work on the footprint of bottom trawling, where around 2% of the total area was trawled in the Aleutian Islands and 45% in the North Sea (Amoroso *et al.* 2018). The exploitation rates in the North Sea showed the most pronounced temporal decline in catch per biomass (i.e., from 0.4 in the 1980s to 0.2 year<sup>-1</sup> in recent years), supporting previous studies documenting a strong reduction of fishing pressure on the demersal community (Couce *et al.* 2020). All North American regions had exploitation rates <0.06 year<sup>-1</sup>. These lower rates, compared with the Northeast Atlantic region, may be due to a different fisheries management strategy (Battista *et al.* 2018) and/or because fewer demersal species are commercially exploited.

We found a strong negative relationship between demersal community biomass and a log<sub>10</sub>-transformed fishing exploitation rate. This implies that small increases at low exploitation rate (based on the untransformed data) may cause large declines in demersal community biomass. We expect that this non-linear effect is caused by the decline of large and long-lived individuals that have accumulated biomass over their lifetime. Additionally, fishing had a weak but negative relationship with the mean trophic level of the community, which in turn had a negative relationship with biomass (see Figure S2.2 for hypothesized mechanisms). This indirect effect of fishing channeled through mean trophic level is thus positive on demersal community biomass but is weaker than the direct negative effect of fishing. The sensitivity of the demersal fish community to fishing highlights that reducing fishing mortality is an effective way of reducing the impacts of climate

change on the fish community, *sensu* Brander (2007). Our results further stress the need for future exploitation rate scenarios in line with the Shared Socioeconomic Pathways for making climate change projections of fish biomass (Hamon *et al.* 2021).

### Demersal and pelagic fish

Changes in community biomass were solely analyzed for the demersal part of the fish community. However, higher proportions of pelagic fish catch relative to demersal fish catch are observed in the three ecoregions with the highest temperatures, i.e. Northern Gulf of Mexico, Carolinian and Floridian. These higher proportions support previously documented patterns in global fish catches towards dominance of pelagic fish towards the tropics (van Denderen *et al.* 2018) and could have contributed to the observed declines of demersal fish biomass with temperature. The trophodynamic model implicitly accommodated regional variation in pelagic and demersal fish (by way of parameter  $p$ ). Although the trophodynamic model confirmed the SEM outcome, it is important to note that not all the decline in demersal fish biomass with temperature should be associated with a direct bioenergetic effect of temperature on fish.

### Conclusion

To anticipate the consequences of climate change on marine ecosystem function and services (e.g., food provisioning and climate regulation through carbon sequestration) it is critical to understand how changes in ocean productivity and temperature may affect the upper trophic levels of marine ecosystems. Our large-scale empirical investigation showed a pronounced latitudinal increase in demersal fish community biomass from the subtropics to the poles. The changes in demersal community biomass are linked to differences in temperature, fishing, and ocean productivity. The observed negative relationship between temperature and community biomass indicates that the long-term impacts of climate warming on community biomass will be negative. This finding is consistent with model predictions of fish biomass (Lotze *et al.* 2019; Tittensor *et al.* 2021). Hence, our results provide an important empirical basis to formally validate and ground truth such model-based predictions in order to evaluate sound and robust management actions in the face of global change.

### Acknowledgement

We wish to thank ICES, NOAA, DFO, IMR and OceanAdapt/Malin Pinsky for making data available and/or accessible. P.D.v.D. was funded by the European Union’s Horizon 2020 research and innovation programme under the Marie Skłodowska-Curie grant agreement No 101024886. M.L. acknowledges financial support from the European Union’s Horizon 2020 projects “Mission Atlantic” (ID: 862428) and “B-USEFUL” (ID: 101059823). KHA acknowledges support from the Danish Research Foundation and from the VKR Centre for Ocean Life. CMP was funded by NOAA grants NA20OAR4310438, NA20OAR4310441, and NA20OAR4310442.

### References

- Amante, C. & Eakins, B. (2009). *ETOPO1 1 arc-minute global relief model: procedures, data sources and analysis* .
- Amoroso, R.O., Pitcher, C.R., Rijnsdorp, A.D., McConnaughey, R.A., Parma, A.M., Suuronen, P., *et al.* (2018). Bottom trawl fishing footprints on the world’s continental shelves. *Proc. Natl. Acad. Sci.* , 115, E10275–E10282.
- Andersen, K.H. (2019). *Fish ecology, evolution, and exploitation* . Princeton University Press.
- Battista, W., Kelly, R.P., Erickson, A. & Fujita, R. (2018). Fisheries Governance Affecting Conservation Outcomes in the United States and European Union. *Coast. Manag.* , 46, 388–452.
- Beukhof, E., Dencker, T.S., Palomares, M.L.D. & Maureaud, A. (2019). A trait collection of marine fish species from North Atlantic and Northeast Pacific continental shelf seas.
- Brander, K.M. (2007). Global fish production and climate change. *Proc. Natl. Acad. Sci.* , 104, 19709–19714.

- Brown, J.H., Gillooly, J.F., Allen, A.P., Savage, V.M. & West, G.B. (2004). Toward a metabolic theory of ecology. *Ecology* , 85, 1771–1789.
- Carl, G. & Kühn, I. (2010). A wavelet-based extension of generalized linear models to remove the effect of spatial autocorrelation. *Geogr. Anal.* , 42, 323–337.
- Carl, G., Levin, S.C. & Kühn, I. (2018). spind: an R Package to Account for Spatial Autocorrelation in the Analysis of Lattice Data. *Biodivers. Data J.* , 6, e20760.
- Cheung, W.W.L., Sarmiento, J.L., Dunne, J., Frölicher, T.L., Lam, V.W.Y., Deng Palomares, M.L., *et al.* (2013). Shrinking of fishes exacerbates impacts of global ocean changes on marine ecosystems. *Nat. Clim. Chang.* , 3, 254–258.
- Couce, E., Schratzberger, M. & Engelhard, G.H. (2020). Reconstructing three decades of total international trawling effort in the North Sea. *Earth Syst. Sci. Data* , 12, 373–386.
- van Denderen, D., Gislason, H., van den Heuvel, J. & Andersen, K.H. (2020). Global analysis of fish growth rates shows weaker responses to temperature than metabolic predictions. *Glob. Ecol. Biogeogr.* , 29, 2203–2213.
- van Denderen, P.D., Lindegren, M., MacKenzie, B.R., Watson, R.A. & Andersen, K.H. (2018). Global patterns in marine predatory fish. *Nat. Ecol. Evol.* , 2, 65–70.
- van Denderen, P.D., Petrik, C.M., Stock, C.A. & Andersen, K.H. (2021). Emergent global biogeography of marine fish food webs. *Glob. Ecol. Biogeogr.* , 30, 1822–1834.
- Eddy, T.D., Bernhardt, J.R., Blanchard, J.L., Cheung, W.W.L., Colléter, M., du Pontavice, H., *et al.* (2021). Energy flow through marine ecosystems: confronting transfer efficiency. *Trends Ecol. Evol.* , 36, 76–86.
- Frainer, A., Primicerio, R., Kortsch, S., Aune, M., Dolgov, A. V, Fossheim, M., *et al.* (2017). Climate-driven changes in functional biogeography of Arctic marine fish communities. *Proc. Natl. Acad. Sci.* , 114, 12202 LP – 12207.
- Free, C.M., Thorson, J.T., Pinsky, M.L., Oken, K.L., Wiedenmann, J. & Jensen, O.P. (2019). Impacts of historical warming on marine fisheries production. *Science (80- )* , 363, 979–983.
- Friedland, K.D., Langan, J.A., Large, S.I., Selden, R.L., Link, J.S., Watson, R.A., *et al.* (2020). Changes in higher trophic level productivity, diversity and niche space in a rapidly warming continental shelf ecosystem. *Sci. Total Environ.* , 704, 135270.
- Friedland, K.D., Stock, C., Drinkwater, K.F., Link, J.S., Leaf, R.T., Shank, B. V, *et al.* (2012). Pathways between primary production and fisheries yields of Large Marine Ecosystems. *PLoS One* , 7, e28945.
- Froese, R. & Pauly, D. (2018). *FishBase World Wide Web electronic publication. www.fishbase.org, version (10/2018).www.fishbase.org* .
- Gillooly, J.F., Brown, J.H., West, G.B., Savage, V.M. & Charnov, E.L. (2001). Effects of size and temperature on metabolic rate. *Science (80- )* , 293, 2248–2251.
- Gislason, H., Collie, J., MacKenzie, B.R., Nielsen, A., Borges, M. de F., Bottari, T., *et al.* (2020). Species richness in North Atlantic fish: Process concealed by pattern. *Glob. Ecol. Biogeogr.* , 29, 842–856.
- Grace, J.B. (2006). *Structural equation modeling and natural systems* . Cambridge University Press, Cambridge, UK.
- Guiet, J., Galbraith, E.D., Bianchi, D. & Cheung, W.W.L. (2020). Bioenergetic influence on the historical development and decline of industrial fisheries. *ICES J. Mar. Sci.* , 77, 1854–1863.
- Hamon, K.G., Kreiss, C.M., Pinnegar, J.K., Bartelings, H., Batsleer, J., Catalán, I.A., *et al.* (2021). Future socio-political scenarios for aquatic resources in Europe: an operationalized framework for marine fisheries

projections. *Front. Mar. Sci.*

Hatton, I.A., Heneghan, R.F., Bar-On, Y.M. & Galbraith, E.D. (2022). The global ocean size spectrum from bacteria to whales. *Sci. Adv.* , 7, eabh3732.

Kwiatkowski, L., Torres, O., Bopp, L., Aumont, O., Chamberlain, M., Christian, J.R., *et al.* (2020). Twenty-first century ocean warming, acidification, deoxygenation, and upper-ocean nutrient and primary production decline from CMIP6 model projections. *Biogeosciences* , 17, 3439–3470.

Laufkötter, C., John, J.G., Stock, C.A. & Dunne, J.P. (2017). Temperature and oxygen dependence of the remineralization of organic matter. *Global Biogeochem. Cycles* , 31, 1038–1050.

Link, J., Overholtz, W., O'Reilly, J., Green, J., Dow, D., Palka, D., *et al.* (2008). The Northeast US continental shelf Energy Modeling and Analysis exercise (EMAX): Ecological network model development and basic ecosystem metrics. *J. Mar. Syst.* , 74, 453–474.

Lotze, H.K., Tittensor, D.P., Bryndum-Buchholz, A., Eddy, T.D., Cheung, W.W.L., Galbraith, E.D., *et al.* (2019). Global ensemble projections reveal trophic amplification of ocean biomass declines with climate change. *Proc. Natl. Acad. Sci.* , 116, 12907–12912.

Maureaud, A., Hodapp, D., van Denderen, P.D., Hillebrand, H., Gislason, H., Spaanheden Dencker, T., *et al.* (2019). Biodiversity–ecosystem functioning relationships in fish communities: biomass is related to evenness and the environment, not to species richness. *Proc. R. Soc. B Biol. Sci.* , 286, 20191189.

Myers, R.A. & Worm, B. (2003). Rapid worldwide depletion of predatory fish communities. *Nature* , 423, 280–283.

O'Connor, M.I., Piehler, M.F., Leech, D.M., Anton, A. & Bruno, J.F. (2009). Warming and resource availability shift food web structure and metabolism. *PLOS Biol.* , 7, e1000178.

Pauly, D. & Christensen, V. (1995). Primary production required to sustain global fisheries. *Nature* , 374, 255.

Petrik, C.M., Stock, C.A., Andersen, K.H., van Denderen, P.D. & Watson, J.R. (2019). Bottom-up drivers of global patterns of demersal, forage, and pelagic fishes. *Prog. Oceanogr.* , 176, 102124.

Petrik, C.M., Stock, C.A., Andersen, K.H., van Denderen, P.D. & Watson, J.R. (2020). Large pelagic fish are most sensitive to climate change despite pelagification of ocean food webs. *Front. Mar. Sci.* , 7, 588482.

Pinsky, M.L., Worm, B., Fogarty, M.J., Sarmiento, J.L. & Levin, S.A. (2013). Marine taxa track local climate velocities. *Science (80-. )* , 341, 1239–1242.

Pomeroy, L.R. & Deibel, D.O.N. (1986). Temperature regulation of bacterial activity during the spring bloom in Newfoundland coastal waters. *Science (80-. )* , 233, 359–361.

du Pontavice, H., Gascuel, D., Reygondeau, G., Stock, C. & Cheung, W.W.L. (2021). Climate-induced decrease in biomass flow in marine food webs may severely affect predators and ecosystem production. *Glob. Chang. Biol.* , 27, 2608–2622.

Rall, B.C., Brose, U., Hartvig, M., Kalinkat, G., Schwarzmüller, F., Vucic-Pestic, O., *et al.* (2012). Universal temperature and body-mass scaling of feeding rates. *Philos. Trans. R. Soc. B Biol. Sci.* , 367, 2923 LP – 2934.

Ricard, D., Minto, C., Jensen, O.P. & Baum, J.K. (2012). Examining the knowledge base and status of commercially exploited marine species with the RAM Legacy Stock Assessment Database. *Fish Fish.* , 13, 380–398.

Rice, J. & Gislason, H. (1996). Patterns of change in the size spectra of numbers and diversity of the North Sea fish assemblage, as reflected in surveys and models. *ICES J. Mar. Sci.* , 53, 1214–1225.

Rosseel, Y. (2012). Lavaan: An R Package for structural equation modeling. *J. Stat. Softw.* , 48, 1–36.

Silsbe, G.M., Behrenfeld, M.J., Halsey, K.H., Milligan, A.J. & Westberry, T.K. (2016). The CAFE model: A net production model for global ocean phytoplankton. *Global Biogeochem. Cycles* , 30, 1756–1777.

Stock, C.A., Dunne, J.P. & John, J.G. (2014). Global-scale carbon and energy flows through the marine planktonic food web: an analysis with a coupled physical–biological model. *Prog. Oceanogr.* , 120, 1–28.

Stock, C.A., John, J.G., Rykaczewski, R.R., Asch, R.G., Cheung, W.W.L., Dunne, J.P., *et al.* (2017). Reconciling fisheries catch and ocean productivity. *Proc. Natl. Acad. Sci.* , 114, E1441–E1449.

Tittensor, D.P., Novaglio, C., Harrison, C.S., Heneghan, R.F., Barrier, N., Bianchi, D., *et al.* (2021). Next-generation ensemble projections reveal higher climate risks for marine ecosystems. *Nat. Clim. Chang.* , 11, 973–981.

Vucic-Pestic, O., Ehnes, R.B., Rall, B.C. & Brose, U. (2011). Warming up the system: higher predator feeding rates but lower energetic efficiencies. *Glob. Chang. Biol.* , 17, 1301–1310.

Walker, N.D., Maxwell, D.L., Le Quesne, W.J.F. & Jennings, S. (2017). Estimating efficiency of survey and commercial trawl gears from comparisons of catch-ratios. *ICES J. Mar. Sci.* , 74, 1448–1457.

Watson, R.A. (2017). A database of global marine commercial, small-scale, illegal and unreported fisheries catch 1950–2014. *Sci. data* , 4, 170039.

Wei, C.-L., Rowe, G.T., Escobar-Briones, E., Boetius, A., Soltwedel, T., Caley, M.J., *et al.* (2011). Global patterns and predictions of seafloor biomass using random forests. *PLoS One* , 5, e15323.

Windle, M.J.S., Rose, G.A., Devillers, R. & Fortin, M.-J. (2010). Exploring spatial non-stationarity of fisheries survey data using geographically weighted regression (GWR): an example from the Northwest Atlantic. *ICES J. Mar. Sci.* , 67, 145–154.

## Figures

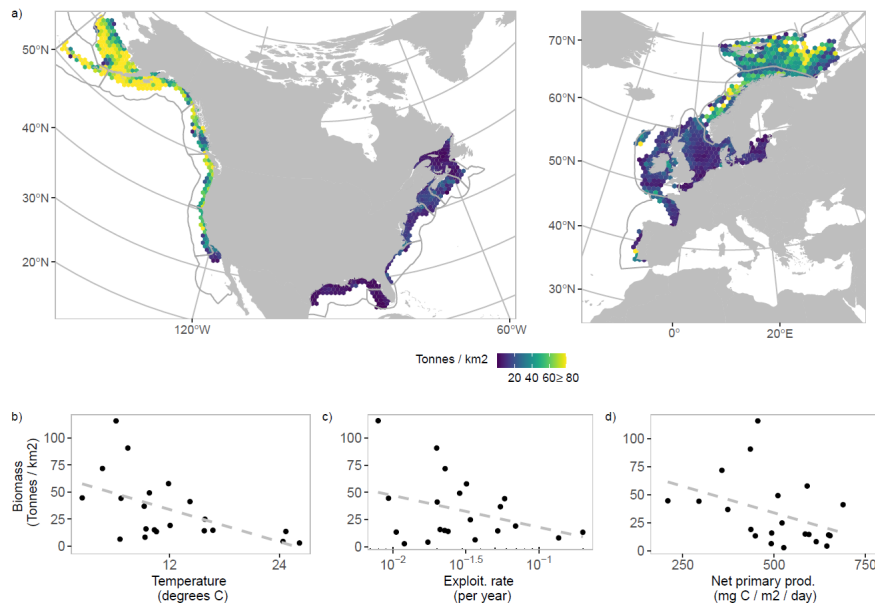


Figure 1. (a) Average demersal fish biomass per grid cell (6000 km<sup>2</sup>) in the different ecoregions between 1990–2015. Bivariate correlations between average demersal fish biomass and temperature (b), exploitation

rate (c) and net primary production (d) aggregated per ecoregion. The lines in the bivariate plots were fit with linear regression.

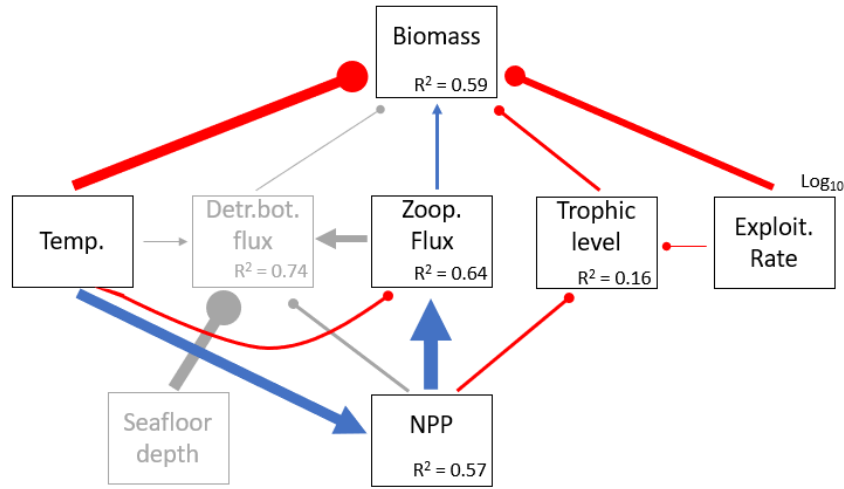


Figure 2. Final structural equation model (SEM) showing the direct and indirect effects of predictors on demersal fish biomass averaged across model runs (conducted at the broader spatial scales for each time period; Figure S2.4). The color and thickness of the arrows shows the sign (blue arrow = positive, red oval = negative) and strength of each relationship based on linear scaling of the mean standardized coefficients across model runs. The coefficient of determination ( $R^2$ ) is also indicated for each response variable. We removed the grey predictor variables and pathways in the final SEM to limit the number of predictors relative to the number of observations and to assess goodness-of-fit.

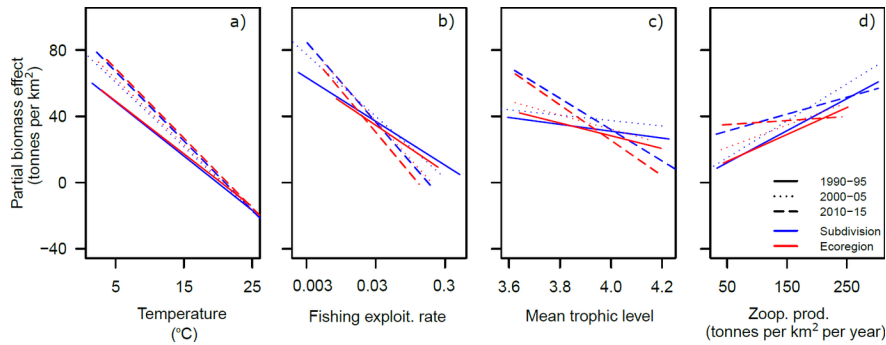


Figure 3. Partial effect of temperature (a), fishing exploitation rate (b), mean trophic level (c) and zooplankton production (d) on demersal fish biomass as estimated from the SEM (Figure 2). The plots show the change in demersal fish biomass along the range of each predictor while keeping the other variables fixed at their mean values. The different lines represent different spatial scales and time periods (see legend and Figure S2.4 for each SEM).

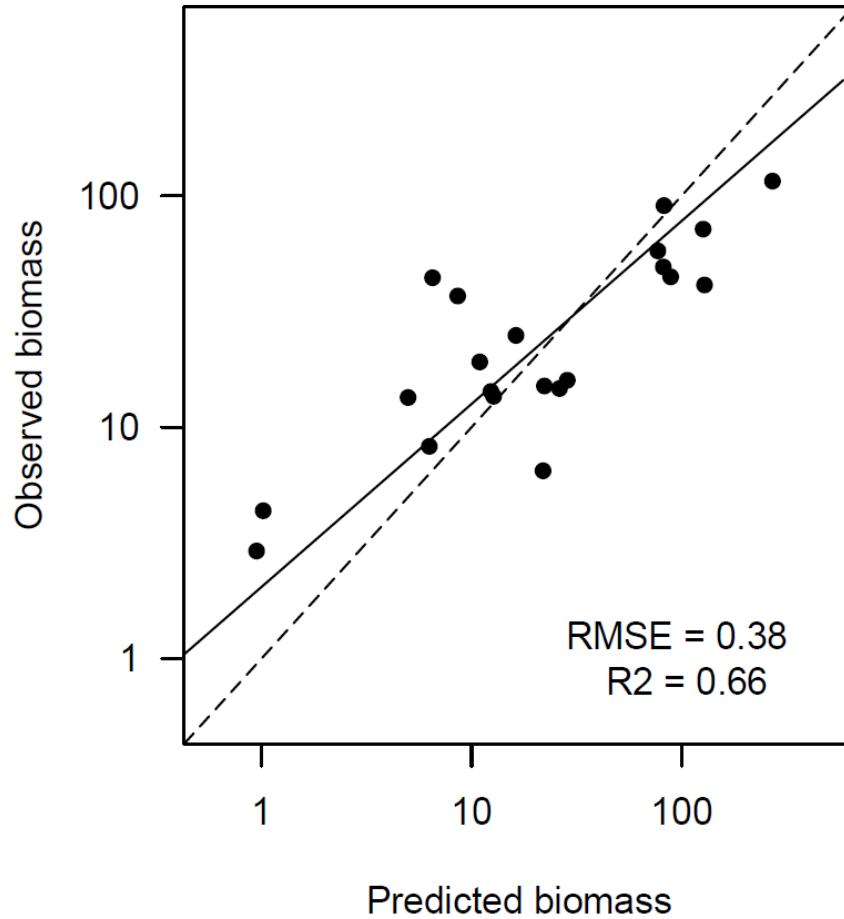


Figure 4. Ecoregion comparison of predicted and observed demersal fish biomass (both in tonnes per km<sup>2</sup>) averaged between 1990-2015. The predicted biomass is estimated using the trophodynamic model with a trophic transfer efficiency of 0.075 and a temperature scaling ( $Q_{10}$ ) of the trophic transfer efficiency of 0.55 (see Figure S2.5 for a range of values). The dashed line is the 1:1 line, and the solid line is a linear fit.  $R^2$  is the coefficient of determination, RMSE the Root Mean Square Error. Similar results are obtained when analysis is done at subdivision scale (Figure S2.6).

Table 1. Analysis of temporal demersal biomass variation in ecoregions with different recursive biomass models and surplus production models. The  $\Delta AIC$  is obtained by subtracting the AIC of a model with a temperature term  $\vartheta T$  from the AIC of a model without this term.

	Formula	Model information	$\vartheta$ estimate ( $\Delta AIC$ )
Recursive biomass models	Recursive biomass models		

	Formula	Model information	$\vartheta$ estimate ( $\Delta AI^*$ )
(M1)	$B_{i,t+1} = (\alpha - \beta B_{i,t} + \theta_i T_{i,t}) B_{i,t} - C_{i,t} + \varepsilon_{i,t}$	Changes in biomass $B$ in ecoregion $i$ over time $t$ depend on biomass in the previous year, a growth term $\alpha$ , a carrying capacity term $\beta$ and $\vartheta$ , which describes the influence of temperature $T$ on the fish community. $C$ is the observed demersal catch and is treated as an offset.	$\vartheta = 0.003$ (2.0)
(M2)	$B_{i,t+1} = \left( \alpha - \beta B_{i,t} - \frac{C_{i,t}}{B_{i,t}} \right) B_{i,t} \bullet e^{T_{i,t} \bullet \varepsilon_{i,t}}$	Same as M1, but now temperature affects the fish community with a multiplicative temperature term.	$\vartheta = 0.012$ (1.9)
(M3)	$B_{i,t+1} = \left( 1 - \frac{C_{i,t}}{B_{i,t}} \right) B_{i,t} \bullet e^{T_{i,t} \bullet \varepsilon_{i,t}}$	Ricker inspired equation with same terms as M1 and M2.	$\vartheta = 0.046$ (-0.1)
Surplus production models	Surplus production models		
(M4)	$P_{i,t} = r_i B_{i,t} \left( 1 - \frac{B_{i,t}}{K_i} \right) \bullet e^{T_{i,t} \bullet \varepsilon_{i,t}}$	Surplus production model with a temperature term following Free et al. (2019). Surplus production $P_{i,t}$ is calculated as the change in total biomass: $P_{i,t} = B_{i,t+1} - B_{i,t} + C_{i,t}$ . $r$ is the intrinsic growth rate and $K$ the carrying capacity. Temperature affects the fish community with a multiplicative temperature term.	$\vartheta = -0.253$ (1.0)
(M5)	$P_{i,t} = r_i B_{i,t} \left( 1 - \frac{B_{i,t}}{K_i \bullet e^{\vartheta T_{i,t}}} \right) + \varepsilon_{i,t}$	Similar to M4, but now temperature only affects the carrying capacity $K$ .	$\vartheta = -0.02$ (1.9)

Table 2. Selected models using wavelet-revised model regression for spatial changes in demersal fish biomass at the grid cell level. The models are tested with all five predictor variables from the original SEM. Mean trophic level is not shown as it is not part of the best candidate model in any of the time periods. Temperature

=  $T$  , fishing exploitation =  $ER$  , zooplankton production =  $Z_{flux}$  and detrital bottom flux =  $D_{flux}$  .

Model estimated intercept	P-value	Years	Nb of grid cells
$\log_{10}(B) = 0.70 - 0.04[?]T - 0.36[?]\log_{10}(ER) + 0.002[?]Z_{flux} + 0.001[?]D_{flux}$	All P <0.001	1990-95	846
$\log_{10}(B) = 1.07 - 0.04[?]T - 0.27[?]\log_{10}(ER) + 0.002[?]Z_{flux} - 0.0003[?]D_{flux}$	$P_{D_{flux}} = 0.008$ All P <0.001	2000-05	983
$\log_{10}(B) = 1.10 - 0.04[?]T - 0.23[?]\log_{10}(ER) + 0.002[?]Z_{flux} - 0.0002[?]D_{flux}$	$P_{D_{flux}} = 0.05$ ; other P <0.001	2010-15	972